J|A|C|S
ARTICLES
Published on Web 04/26/2006

Photoreversible DNA Condensation Using Light-Responsive Surfactants

Anne-Laure M. Le Ny and C. Ted Lee, Jr.*

Contribution from the Department of Chemical Engineering and Material Sciences, University of Southern California, Los Angeles, California 90089-1211

Received November 18, 2005; E-mail: tedlee@usc.edu

Abstract: A means to control DNA compaction with light illumination has been developed using the interaction of DNA with a photoresponsive cationic surfactant. The surfactant undergoes a reversible photoisomerization upon exposure to visible (trans isomer, more hydrophobic) or UV (cis isomer, more hydrophilic) light. As a result, surfactant binding to DNA and the resulting DNA condensation can be tuned with light. Dynamic light scattering (DLS) measurements were used to follow λ-DNA compaction from the elongated-coil to the compact globular form as a function of surfactant addition and light illumination. The results reveal that compaction occurs at a surfactant-to-DNA base pair ratio of approximately 7 under visible light, while no compaction is observed up to a ratio of 31 under UV light. Upon compaction, the measured diffusion coefficient increases from a value of 0.6×10^{-8} cm^2/s (elongated coil with an end-to-end distance of 1.27 μm) to a value of 1.7×10^{-8} cm^2/s (compact globule with a hydrodynamic radius of 120 nm). Moreover, the light-scattering results demonstrate that the compaction process is completely photoreversible. Fluorescence microscopy with T4-DNA was used to further confirm the light-scattering results, allowing single-molecule detection of the light-controlled coil-to-globule transition. These structural studies were combined with absorbance and fluorescence spectroscopy of crystal violet in order to elucidate the binding mechanism of the photosurfactant to DNA. The results indicate that both electrostatic and hydrophobic forces are important in the compaction process. Finally, a DNA−photosurfactant−water phase diagram was constructed to examine the effects of both DNA and surfactant concentration on DNA compaction. The results reveal that precipitation, which occurs during the latter stages of condensation, can also be reversibly controlled with light illumination. The combined results clearly show the ability to control the interaction between DNA and the complexing agent and, therefore, DNA condensation with light.

Introduction

Complexing agents such as cationic surfactants,[1−7] and lipids,[8,9] neutral and cationic polymers,[10−13] multivalent ions,[14−19] and alcohols[20−22] have been shown to condense DNA from an extended, wormlike conformation into a variety of compact structures (e.g., toroids, spheroids, and rods[15,23,24]) analogous to the conformation of DNA in virus heads. Depending on the

(1) Llères, D.; Clamme, J.-P.; Dauty, E.; Blessing, T.; Krishnamoorthy, G.; Duportail, G.; Mély, Y. Investigation of the stability of dimeric cationic surfactant/DNA complexes and their interaction with model membrane systems. *Langmuir* **2002**, *18*, 10340−10347.
(2) Guillot, S.; McLoughlin, D.; Jain, N.; Delsanti, M.; Langevin, D. Polyelectrolyte−surfactant complexes at interfaces and in bulk. *J Phys.: Condens. Matter* **2003**, *15*, S219−S224.
(3) Dias, R.; Mel'nikov, S.; Lindman, B.; Miguel, M. G. DNA phase behavior in the presence of oppositely charged surfactants. *Langmuir* **2000**, *16*, 9577−9583.
(4) Mel'nikov, S. M.; Sergeyev, V. G.; Yoshikawa, K. Discrete coil−globule transition of large DNA induced by cationic surfactant. *J. Am. Chem. Soc.* **1995**, *117*, 2401−2408.
(5) Gorelov, A. V.; Kudryashov, E. D.; Jacquier, J.-C.; McLoughlin, D. M.; Dawson, K. A. Complex formation between DNA and cationic surfactant. *Physica A* **1998**, *249*, 216−225.
(6) Miguel, M. G.; Pais, A. A. C. C.; Dias, R. S.; Leal, C.; Rosa, M.; Lindman, B. DNA−cationic amphiphile interactions. *Colloids Surf., A* **2003**, *228*, 43−55.
(7) Bathaie, S. Z.; Moosavi-Movahedi, A. A.; Saboury, A. A. Energetic and binding properties of DNA upon interaction with dodecyl trimethylammonium bromide. *Nucleic Acids Res.* **1999**, *27* (4), 1001−1005.
(8) Felgner, P. L.; Gadek, T.; Holm, M.; Roman, R.; Chan, H.; Wenz, M.; Northrop, J.; Ringold, G.; Danielson, M. Lipofection: A highly efficient, lipid-mediated DNA-transfection procedure. *Proc. Natl. Acad. Sci. U.S.A.* **1987**, *84*, 7413−7417.
(9) Mahato, R. I.; Rolland, A.; Tomlinson, E. Cationic lipid-based gene delivery systems: pharmaceutical perspectives. *Pharm. Res.* **1997**, *14* (7), 853−859.
(10) Gershon, H.; Ghirlando, R.; Guttman, S. B.; Minsky, A. Mode of formation and structural features of DNA−cationic liposome complexes used for transfection. *Biochemistry* **1993**, *32*, 7132−7151.
(11) Yoshikawa, K. Controlling the higher-order structure of giant DNA molecules. *Adv. Drug Delivery Rev.* **2001**, *52*, 235−244.
(12) Huang, W.; Zhang, Z.; Han, X.; Tang, J.; Wang, J.; Dong, S.; Wang, E. Liposome-mediated conformation transition of DNA detected by molecular probe: Methyl green. *Bioelectrochemistry* **2003**, *59*, 21−27.
(13) Minnagawa, K.; Matsuzawa, Y.; Yoshikawa, K.; Khokhlov, A. R.; Doi, M. Direct observation of the coil−globule transition in DNA molecules. *Biopolymers* **1994**, *34*, 555−558.
(14) He, S.; Arscott, P. G.; Bloomfield, V. A. Condensation of DNA by multivalent cations: Experimental studies of condensation kinetics. *Biopolymers* **2000**, *53*, 329−341.
(15) Bloomfield, V. A. DNA Condensation by multivalent cations. *Biopolymers* **1997**, *44* (3), 269−282.
(16) Cárdenas, M.; Schillén, K.; Nylander, T.; Jansson, J.; Lindman, B. DNA Compaction by cationic surfactant in solution and at polystyrene particle solution interfaces: a dynamic light scattering study. *Phys. Chem. Chem. Phys.* **2004**, *6*, 1603−1607.
(17) Widom, J.; Baldwin, R. L. Inhibition of cation-induced DNA condensation by intercalating dyes. *Biopolymers* **1983**, *22*, 1621−1632.
(18) Vijayanathan, V.; Thomas, T.; Shirahata, A.; Thomas, T. J. DNA condensation by polyamines: A laser light scattering study of structural effects. *Biochemistry* **2001**, *40*, 13644−13651.
(19) Bustamante, C.; Housel, T. W.; Beach, D. A.; Maestre, M. F. Fluorescence microscopy of the dynamics of supercoiling, folding and condensation of bacterial chromosomes, induced by acridine orange. *J. Biomol. Struct. Dyn.* **1990**, *8* (3), 643−655.

10.1021/ja0576738 CCC: $33.50

type of condensing agent, compaction can occur by several mechanisms, including neutralization of the phosphate charges and/or reorientation of the water dipoles near DNA surfaces leading to suppression of intramolecular electrostatic repulsive forces or modification of the solvent properties giving rise to unfavorable interactions between the solvent and DNA. In the case of compaction induced by cationic ions through a reduction of intramolecular electrostatic forces, approximately 90% of the DNA charges must be neutralized for condensation to occur.[15] When this neutralization and condensation is induced by cationic surfactants, a combination of hydrophobic as well as electrostatic forces must be considered. For example, condensation has been found to occur at lower surfactant concentrations as the length of the hydrocarbon tail of the surfactant and, thus, the magnitude of hydrophobic forces, is increased.[18] This suggests the possibility of using photoresponsive surfactants to induce DNA condensation, where light can be used to control surfactant hydrophobicity, as discussed below.

DNA condensation is relevant from the point of view of gene therapy, where it has been shown that complexation and the resulting compaction are essential to protect DNA from nuclease,[15] and to allow entry of DNA into cells, mainly by the endocytic pathway.[25] Indeed, this method is preferred over viral delivery vectors, due to the potential for immunological responses associated with the use of viruses. However, while complexing agents can increase *cellular uptake* as a result of DNA neutralization and compaction, the tight binding of these same agents to DNA may also generally preclude or greatly reduce *nuclear uptake*, resulting in lower transfection efficiencies compared to viral vectors. This occurs because, in the condensed state, the interaction of DNA with intracellular molecules such as importin or transportin, which transport DNA into the nucleus, is largely prevented.[26,27] Indeed, it has been shown that vector unpacking can be a limiting barrier to gene delivery.[28,29] Thus, the development of photoreversible DNA complexes could greatly increase transfection efficiency. In addition, the ability to control DNA condensation with simple light illumination could find widespread use in areas such as biotechnology (DNA microarrays, scaffolds, molecular machines) and DNA-based chemistry.

In an attempt to develop *reversible* DNA compaction, in the present work we demonstrate that the interaction of a light-sensitive cationic surfactant with DNA can allow for DNA condensation (or expansion) to be initiated with light illumination. The azobenzene trimethylammonium bromide surfactant, similar to surfactants used to reversibly photocontrol the folding of proteins (e.g., bovine serum albumin[30] and lysozyme[31]), adopts a relatively hydrophobic trans configuration in visible light or dark conditions, while photoisomerizing to a relatively hydrophilic cis conformation in UV light (365 nm). As a consequence, under visible light the trans isomer preferentially binds to oppositely charged DNA, decreasing intramolecular electrostatic repulsions and leading to DNA compaction, while exposure to UV light causes the surfactant to dissociate from DNA, returning the DNA molecule to the expanded-coil structure. For the larger DNA molecules used in this study, dynamic light scattering (λ-DNA) and fluorescence microscopy (T4-DNA) are employed to directly detect light-initiated coil $\leftrightarrow$ globule transitions. In addition, UV−vis absorbance and fluorescence are used to investigate the molecular mechanisms responsible for DNA condensation.

Dynamic Light Scattering (DLS). Dynamic light scattering is a nondestructive, nonintrusive technique that has been extensively used to measure the dynamics of polymers[32−35] and polyelectrolytes[36−38] in solution. The DLS technique has also been applied to DNA solutions;[14,16,17,21,39−45] however, in this case analysis of the results is complicated by the dynamical behavior of DNA molecules. For example, in the elongated-

(20) Mikhailenko, S. V.; Sergeyev, V. G.; Zinchenko, A. A.; Gallyamov, M. O.; Yaminsky, I. V.; Yoshikawa, K. Interplay between folding/unfolding and helix/coil transitions in giant DNA. *Biomacromolecules* **2000**, *1*, 597−603.
(21) Roy, K. B.; Anthony, T.; Saxena, A.; Bohidar, H. B. Ethanol-induced condensation of calf thymus DNA studied by laser light scattering. *J. Phys. Chem. B* **1999**, *103*, 5117−5121.
(22) Yoshikawa, K.; Yoshikawa, Y.; Koyama, Y.; Kanbe, T. Highly effective compaction of long duplex DNA induced by poly(ethylene glycol) with pendant amino groups. *J. Am. Chem. Soc.* **1997**, *119*, 6473−6477.
(23) Yoshikawa, Y.; Yoshikawa, K.; Kanbe, T. Formation of giant toroid from long duplex DNA. *Langmuir* **1999**, *15*, 4085−4088.
(24) Arscott, P. G.; Ma, C.; Wenner, J. R.; Bloomfield, V. A. DNA condensation by cobalt hexaammine (III) in alcohol−water mixtures: dielectric constant and other solvent effects. *Biopolymers* **1995**, *36* (3), 345−364.
(25) Remy-Kristensen, A.; Clamme, J.-P.; Vuilleumier, C.; Duportail, G.; Khury, J.-G.; Mély, Y. Role of endocytosis in the transfection of L929 fibroblasts by polyethylenimine/DNA complexes. *Biochim. Biophys. Acta* **2001**, *1514* (1), 21−32.
(26) Xu, Y.; Szoka, F. C., Jr. Mechanism of DNA release from cationic/DNA complexes used in cell transfection. *Biochemistry* **1996**, *35*, 5616−5623.
(27) Lechardeur, D.; Lukacs, G. L. Intracellular barriers to nonviral gene transfer. *Curr. Gene Ther.* **2002**, *2*, 183−194.
(28) Schaffer, D. V.; Fidelman, N. A.; Dan, N.; Lauffenburger, D. A. Vector unpacking as a potential barrier for receptor-mediated polyplex gene delivery. *Biotechnol. Bioeng.* **2000**, *67*, 598−606.
(29) Read, M. L.; Bremner, K. H.; Oupicky, D.; Green, N. K.; Searle, P. F.; Seymour, L. W. Vectors based on reducible polycations facilitate intracellular release of nucleic acid. *J. Gene Med.* **2003**, *5*, 232−245.
(30) Lee, C. T., Jr.; Smith, K. A.; Hatton, T. A. Photocontrol of protein folding: The interaction of photoresponsive surfactants with bovine serum albumine. *Biochemistry* **2005**, *44* (2), 524−536.
(31) Hamill, A.; Lee, C. T., Jr. Probing lysozyme conformation with light reveals a new folding intermediate. *Biochemistry* **2005**, *44*, 15139−15149.
(32) Delong, L. M.; Russo, P. S. Thermodynamic and dynamic behavior of semi flexible polymers in the isotropic phase. *Macromolecules* **1991**, *24*, 16139−16155.
(33) Oyama, Y.; Takada, A.; Nemeto, N. Depolarized dynamic light scattering of rodlike molecules. *Nihon Reoroji Gakkaishi* **1999**, *27* (4), 249−250.
(34) Mathiez, P.; Mouttet, C.; Weisbuch, G. Quasielastic light-scattering study of polyadenylic acid solutions. II. *Biopolymers* **1981**, *20*, 2381−2394.
(35) Phalakornkul, J. K.; Gast, A. P.; Pecora, R. Rotational and translational dynamics of rodlike polymers: A combined transient electric birefringence and dynamic light scattering study. *Macromolecules* **1999**, *32* (9), 3122−3135.
(36) Sedlak, M. Structure and dynamics of polyelectrolytes solutions by light scattering. In *Physical Chemistry of Polyelectrolytes*; Radeva, T., Ed.; Marcel Dekker, Inc.: New York, 2001; pp 1−58.
(37) Liu, H.; Skibinska, L.; Gapinski, J.; Patkowski, A.; Fischer, E. W.; Pecora, R. Effect of electrostatic interactions on the structure and dynamics of a model polyelectrolyte. I. Diffusion. *J. Chem. Phys.* **1998**, *109* (17), 7556−7566.
(38) Skibinska, L.; Gapinski, J.; Liu, H.; Patkowski, A.; Fisher, E. W.; Pecora, R. Effect of electrostatic interactions on the structure and dynamics of a model polyelectrolyte. II. Intermolecular correlations. *J. Chem. Phys.* **1999**, *110* (3), 1794−1800.
(39) Borsali, R.; Nguyen, H.; Pecora, R. Small-angle neutron scattering and dynamic light scattering from a polyelectrolyte solution: DNA. *Macromolecules* **1998**, *31*, 1548−1555.
(40) Allison, S. A.; Sorlie, S. S.; Pecora, R. Brownian dynamics simulations of wormlike chains: dynamic light scattering from a 2311 base pair DNA fragment. *Macromolecules* **1990**, *23*, 1110−1118.
(41) Lehner, D.; Lindner, H.; Glatter, O. Determination of the translational and rotational diffusion coefficients of rodlike particles using depolarized dynamic light scattering. *Langmuir* **2000**, *16*, 1689−1695.
(42) Kam, Z.; Borochov, N.; Eisenberg, H. Dependence of laser light scattering of DNA on NaCl concentration. *Biopolymers* **1981**, *20*, 2671−2690.
(43) Hopman, P. C.; Koopman, G.; Greve, J. Influence of double scattering in determination of rotational diffusion coefficients by depolarized dynamic light scattering: application to the bacteriophages T7 and T4B. *Biopolymers* **1980**, *19*, 1241−1255.
(44) Langowski, J.; Giesen, U.; Lehmann, C. Dynamics of superhelical DNA studied by photon correlation spectroscopy. *Biophys. Chem.* **1986**, *25*, 191−200.
(45) Thomas, T. C.; Allison, S. A.; Schurr, J. M. Dynamic light scattering studies of internal motions in DNA II. Clean viral DNAs. *Biopolymers* **1980**, *19*, 1451−1474.

coil state, DNA molecules will undergo translational and rotational diffusion, internal diffusive modes due to macromolecular flexibility, and possible intramolecular interference effects for larger DNA molecules with characteristic sizes similar to the wavelength of light.[46] Each of these effects is detected in a light-scattering experiment, meaning that careful examination of the data is required for quantitative analysis.

For example, the normalized correlation function $g^{(1)}$ for optically isotropic rods undergoing combined (decoupled) translational and rotational diffusion, as well as internal motions due to flexibility, etc., can be represented by a sum of exponential decays

$$g^{(1)}(q,\tau) = S_0(ql)\exp(-D_T q^2 \tau) + S_1(ql)\exp[(-D_T q^2 - 6D_R)\tau] + \text{internal modes} \quad (1)$$

where l is the length of the rod, D_T is the translational diffusion coefficient, τ is the relaxation time, D_R is the rotational diffusion coefficient, $S_0(ql)$ and $S_1(ql)$ are the scattering amplitudes, and q is the scattering vector defined as

$$q = \frac{4\pi n}{\lambda}\sin\left(\frac{\theta}{2}\right) \quad (2)$$

where n is the refractive index of the solvent, λ the wavelength of light, and θ the scattering angle. This expression has been used in a variety of DNA-based systems,[32,39,47] especially for relatively small DNA molecules (<1000 bp) where the internal-modes term (i.e., flexibility) can be ignored.[48,49] In the case of larger DNA molecules, however, such as λ-DNA employed in the present study, macromolecular flexibility could be expected to contribute to the scattering data. Indeed, the root mean square end-to-end distance ($\langle R^2\rangle^{1/2}$) of λ-DNA can be estimated from the expression[50]

$$\langle R^2\rangle = 2LP[1 - P/L + (P/L)\exp(-L/P)] \quad (3)$$

where L is the contour length (16.3 μm)[51] and P is the persistence length (50 nm),[50] equating to an end-to-end distance for λ-DNA of 1.27 μm. Thus, due to this high ratio of contour length versus persistence length, λ-DNA should be considered to be quite flexible, giving rise to an internal-modes term in eq 1 (see also Figure 2). Furthermore, because of the expanded-coil shape of λ-DNA, rotational diffusion would also be expected to contribute to the correlation function.

Thus, for relatively large DNA molecules it becomes challenging to extract the translational diffusion coefficient D_T from the correlation function as a means of estimating molecular size (through either the Stokes−Einstein equation for spheres, $D_T = k_B T/6\pi\eta R_H$, where k_B is the Boltzmann constant, T is temperature, η is solvent viscosity, and R_H is the hydrodynamic radius, or from Tirado and de la Torre's equation for rods,[52] $D_T = k_B T[\ln(l/d) + \gamma]/3\pi\eta l$, where d is the diameter and l is the length of the rod, while γ is given as a function[39] of d and l). Fortunately, each term in eq 1 has a different angular dependence, providing a convenient means to enhance the contribution of translational motion to the overall scattering intensity, as will be discussed below.

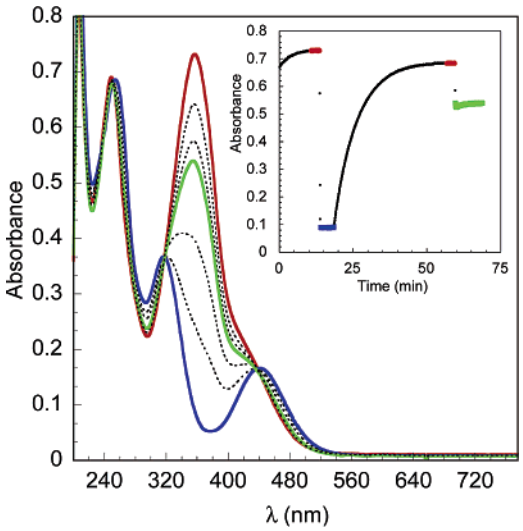

Figure 1. UV−vis absorption spectra of a 31.1 μM azoTAB and 25.6 μM herring testes DNA solution in TE buffer using a 1 cm path length cuvette. The insert shows the isomerization kinetics between the trans and cis forms in the dark (red curve) and under UV (blue curve) light illumination, as well as in visible light conditions (green curve) while being continuously stirred.

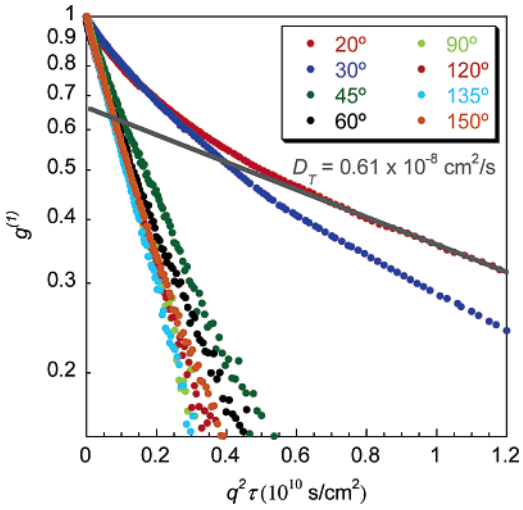

Figure 2. Normalized correlation functions of λ-DNA (0.05 mM) in TE buffer as a function of scattering angle. The translational diffusion coefficient of DNA can be estimated as the slope of the correlation function in the "slow mode" regime at a scattering angle of 20° (see eq 1). Actual values reported for the diffusion coefficient were obtained from the NNLS routine.

Experimental Section

Materials. An azobenzene trimethylammonium bromide surfactant (azoTAB) of the form below was synthesized according to published procedures[53] and purified by recrystallization from ethanol. This

(46) Zero, K. M.; Pecora, R. Rotational and translational diffusion in semidilute solutions of rigid-rod macromolecules. *Macromolecules* **1982**, *15*, 87−93.
(47) Liu, H.; Gapinski, J.; Skibinska, L.; Patkowski, A.; Pecora, R. Effect of electrostatic interactions on the dynamic of semi flexible monodisperse DNA fragments. *J. Chem. Phys.* **2000**, *113* (14), 6001−6010.
(48) Sorlie, S. S.; Pecora, R. A dynamic light scattering study of four DNA restriction fragments. *Macromolecules* **1990**, *23*, 487−497.
(49) Goinga, H. T.; Pecora, R. Dynamics of low molecular weight DNA fragments in dilute and semidilute solutions. *Macromolecules* **1991**, *24*, 6128−6138.
(50) Bloomfield, V. A.; Crothers, D. M.; Tinico, I., Jr. *Physical Chemistry of Nucleic Acids*; Harpers and Row: New York, 1974.
(51) Bustamante, C.; Marko, J. F.; Siggia, E. D.; Smith, S. Entropic elasticity of λ-phage DNA. *Science* **1994**, *265* (5178), 1599−1600.
(52) Tirado, M. M.; de la Torre, J. G. Translational friction coefficients of rigid, symmetric top macromolecules. Application to circular cylinders. *J. Chem. Phys.* **1979**, *71* (6), 2581−2587.
(53) Hayashita, T.; Kurosawa, T.; Miyata, T.; Tanaka, K.; Igawa, M. Effect of structural variation within cationic azo-surfactant upon photoresponsive function in aqueous solution. *Colloid Polym. Sci.* **1994**, *272*, 1611−1616.

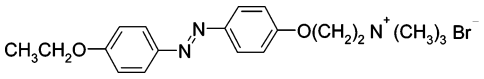

surfactant is similar to azoTAB surfactants used to photocontrol the folding of BSA[30] and lysozyme,[31] modified by the addition of a second aryl ether linkage located on the benzene ring furthest from the charged headgroup. The surfactant undergoes a reversible photoisomerization when exposed to different wavelengths of light, as seen in Figure 1.

In the dark, the surfactant is primarily in the trans, more hydrophobic state (dipole moment across the azo linkage ~0.5 D), whereas with UV light (365 nm) illumination the surfactant converts primarily to the more hydrophilic cis isomer (~3.1 D).[54] Conversion from the cis state to the trans state can be achieved in about 40 min by simply placing the sample in the dark, or alternatively, exposure to visible light (434 nm) illumination can be used to achieve an approximately 70/30 trans/cis photoequilibrium in ~1 min (data not shown). Two illumination methods were used to convert the surfactant to the cis isomer. Prior to DLS and spectroscopic measurements, solutions were exposed to an 84 W long wave UV lamp-365 nm (Spectroline, model no. XX-15A). To maintain the cis form during DLS measurements, the samples were continuously illuminated with a 200 W mercury arc lamp (Oriel, model no. 6283) with a 320 nm band-pass filter (Oriel, model no. 59800). A heat-absorbing filter (Oriel, model no. 59060) was placed in the beam path to absorb IR light produced by the lamp. The combined use of these filters effectively isolates the 365 nm line (UV-A) of the mercury lamp. Exposure of DNA samples to this light source did not result in strand separation or cleavage, as checked through UV−vis absorbance at 260 nm and light-scattering experiments. When needed, a liquid light guide (Oriel, model no. 77557) with a fiber-bundle focusing assembly (Oriel, model no. 77800) was used. The samples were left in room light overnight to convert back to the predominantly trans form.

λ-Phage DNA with a molecular weight of 31.5×10^6 Da (48 502 bp) was purchased from Fermentas (cat. no. SD0011) and used as received for the DLS measurements. The DNA solution was mixed with azoTAB surfactant in a 10 mM Tris, 1 mM EDTA buffer solution (pH 7.5) to a DNA concentration of 0.033 mg/mL. TE buffer was prepared by diluting a 50× TE buffer (USB Corp.) with deionized water (Milli-Q) and was filtered through a 0.2 μm PVDF filter (Whatman) prior to addition to DNA.

The azobenzene surfactant stock solution in TE buffer was also filtered through a 0.2 μm PVDF filter. The surfactant concentration was determined with UV−vis spectroscopy using an extinction coefficient of 24 900 L mol^{-1} cm^{-1} determined at $\lambda_{max} = 357$ nm. Due the size of λ-phage DNA, the molecule is very sensitive to shearing forces. Thus, to prevent cleavage of DNA strands, wide-mouth pipet tips were used, and the solutions once containing DNA were not filtered. Extreme caution was taken while preparing the samples to avoid dust contamination. Indeed, the scattering due to the presence of dust becomes particularly severe especially at low angles,[14,41] and the preparation of dust-free samples is crucial for high-accuracy DLS measurements. Thus, solutions were prepared by adding the desired amount of DNA to filtered surfactant and buffer solutions in precleaned borosilicate tubes stoppered with polyethylene caps (since dust is electrostatically attracted to water) and were left without mixing to equilibrate. The solutions reached equilibrium after 48 h as determined with diffusion coefficient measurements (as discussed below).

Herring testes DNA, type XIV, containing 6.2% sodium salt and purchased from Sigma (D-6898) was used for the determination of the DNA−surfactant−water phase behavior and the spectroscopic experiments. The molecular weight was determined by gel electrophoresis to be polydisperse, covering the broad range less than 1500 bp.

Dynamic Light Scattering. Dynamic light scattering measurements were performed at 25 °C on a Brookhaven model BI-200SM instrument (Brookhaven Instrument Corp.) equipped with a BI-9000AT digital correlator (Brookhaven Instrument Corp.), a 35 mW (Melles Griot, model no. 05-LHP-928) HeNe (632.8 nm) laser, and an avalanche photodiode detector (BI-APD). The scattered light was collected at a low scattering angle of 20° to decrease the contribution of the rotational/internal motions of the DNA molecule (as discussed below). A DNA concentration of $C = 0.033$ mg/mL was used in order to achieve a reasonably high scattering intensity and permit DLS measurements of λ-DNA solutions. Estimating the overlap concentration as $C^* = M_W/N_A(<R^2>^{1/2})^3$, where M_W represents the molecular weight and N_A is Avogadro's number, the concentration used in this study is slightly (~30%) larger than C^*. While working at concentration significantly higher than C^* has been reported to induce the formation of clusters and networks between the DNA chains,[14] this does not appear to be the case in the present study, as the value obtained for the diffusion coefficient of pure λ-DNA is in good agreement with the literature (discussed below). Note that the overlap concentration would be expected to be significantly higher with DNA in the compacted state.

The data were analyzed with the nonnegative least-squares (NNLS) routine. Typically, from 4 to 10 runs were measured for each solution, with the average of all the runs reported. The error bars represent the standard deviation of the measurements. The count rate of scattered light and the baseline of the correlation functions were closely watched throughout the measurement, as both of these undergo erratic fluctuations in the presence of dust. During the compaction process, a dramatic increase of the scattered intensity was observed, requiring the use of either a 10% or 1% neutral density filter placed in front of the incident light to avoid saturation of the detector. To reduce the contributions of faster motions, a vertical polarizer was placed in front of the detector[55] (I_{VV} mode) to suppress the depolarized intensity of the scattered light (I_{VH}).[56]

At the higher ratios of surfactant to DNA base pairs, a small amount of insoluble precipitate was observed under visible light, as expected since DNA neutralization with a cationic surfactant would lead to a reduction in both intramolecular (compaction) and intermolecular (phase separation) electrostatic repulsive forces. In these cases, the solutions were allowed to settle and equilibrate for 48 h, during which time the measured diffusion coefficient of the compacted DNA complex was observed to steadily increase until reaching a constant value. Centrifugation of solutions equilibrated in this manner was found to not affect the measured diffusion coefficients.

Fluorescence Microscopy. T4-phage DNA, 165.6 kilobase pairs (1.076×10^8 Da), was purchased from Wako Chemical (cat. no. 318-03971) and visualized through the use of the fluorescent dye YOYO-3 ($\lambda^{ex}/\lambda^{em} = 612/631$ nm), purchased from Molecular Probes (cat. no. Y3606). 2-Mercaptoethanol (ME), purchased from EM Science, was used as a free radical scavenger to reduce fluorescence fading and photocleavage of the DNA molecules upon exposure to the excitation source. All products were used without further purification. Samples were observed with an Olympus IX71 inverted fluorescence microscope equipped with a 100× oil-immersed objective lens (UPlanFl, N. A. = 1.3) and a U-N31004 TXRD C55480 filter cube. Images were recorded with a Hamamatsu digital CCD camera (model no. C4742-95). To further reduce the light-induced damage to DNA molecules, a 20% neutral density filter was placed in front of the excitation source.

The concentrated DNA solution was diluted to approximately 0.6 μM (base pair) in 0.5× TBE buffer (45 mM Tris, 45 mM borate, 1 mM EDTA) and gently mixed with the dye solution to a ratio of eight base pairs per dye molecule and ME at 4% v/v. Surfactant solution was then immediately added to the desired concentration. Samples were gently mixed by inversion and separated in two fractions, the first one

(54) Shang, T.; Smith, K. A.; Hatton, T. A. Photoresponsive surfactants exhibiting unusually large, reversible surface tension changes under varying illumination conditions. *Langmuir* **2003**, *19*, 10764−10773.

(55) Eimer, W.; Pecora, R. Rotational and translational diffusion of short rodlike molecules in solution: Oligonucleotides. *J. Chem. Phys.* **1991**, *94* (3), 2324−2329.

(56) Pecora, R. *Dynamic Light Scattering. Applications of Photon Correlation Spectroscopy*; Plenum Press: New York and London, Stanford, CA, 1985.

placed in the dark and the second one illuminated with the long wave UV lamp-365 nm. Both fractions were allowed to equilibrate for at least 30 min prior to observation.

Phase Behavior. Herring testes DNA was dissolved in deionized water overnight, and the concentration was measured spectroscopically using the molar extinction coefficient of 6600 M^{-1} cm^{-1}. Samples were prepared by weight, adding the desired amount of DNA and surfactant stock solutions with water in sealed borosilicate test tubes. The solutions were mildly stirred for 48 h and left to equilibrate for another 48 h without mixing. The presence of a solid precipitate was then visually detected. Similar solutions were prepared and immediately placed under UV light, followed by 48 h of stirring and left to equilibrate without mixing for another 48 h.

UV−Vis and Fluorescence Spectroscopy. Absorption measurements were performed on an Agilent model 8453 UV−vis spectrophotometer using 1 cm path length cuvettes. When employed, a crystal violet (Sigma) concentration of 5.2 μM, with a herring testes DNA base pair concentration of 40.8 μM, was used. Crystal violet exhibits a maximum absorbance at 590 nm in water,[57] separated far enough from the absorbance of azoTAB to be readily detected.[58] Fluorescence emission measurements of crystal violet, excited at 570 nm with excitation and emission slit widths of 4 nm, were performed on a QuantaMaster spectrofluorometer, model QM-4 (Photon Technology International) at 25 °C.

Results and Discussion

Pure λ-DNA Solutions. The normalized correlation function measured for a pure λ-DNA solution is shown in Figure 2, illustrating the angular dependence of the various relaxation modes (i.e., translational, rotational, and internal modes as in eq 1).

As detailed by Pecora, it is possible to extract the value of the translational diffusion coefficient at low angles since the effects of both rotational diffusion[59] and flexibility[60] (i.e., internal modes) diminish as q approaches zero (i.e., low scattering angle). Specifically, for $ql < 3$ (where l is approximated as the root mean square end-to-end distance of the DNA under study), rotation accounts for <1% and flexibility accounts for <5% of the scattering intensity, while both of these effects dramatically increase (eventually dominating the scattering intensity) as ql is increased. For example, at the larger angles in Figure 2 (i.e., 45−150°, where $ql = 12.8-32.4$), only a "fast" relaxation mode is evident, as the majority of the scattering intensity originates from rotation and intramolecular flexibility contributions. However, as the scattering angle is reduced to 20°, a "slow" relaxation mode representing translational diffusion becomes detectible. At this scattering angle ($ql = 5.8$), rotation and flexibility are predicted to account for ca. 16% and 26% of the scattering intensity,[59,60] respectively, indicating that the majority of the scattering is indeed from translational diffusion. Therefore, from the slope of the correlation function (see eq 1), the translational diffusion coefficient can be estimated to be approximately 0.61×10^{-8} cm^2/s. This is in good agreement with the value of 0.55×10^{-8} cm^2/s calculated for λ-DNA from the empirical equation of Stellwagen and Stellwagen[61] ($D_T = 7.73 \times 10^{-6} \times N^{-0.672}$ cm^2/s, where N is the number of base pairs) obtained by compiling data from several techniques for a wide range of DNA sizes (10−50 000 bp). Furthermore, Widom and Baldwin suggest a value of 0.53×10^{-9} cm^2/s for λ-DNA in solution.[62] Thus, it appears that a scattering angle of 20° allows accurate measurement of the translational diffusion coefficient of λ-DNA.

Note that to achieve the oft-reported value of $ql < 3$ for λ-DNA would require a scattering angle of ~10° using a HeNe laser (632.8 nm). However, since the presence of even a small amount of dust begins to dominate the scattering at low angles, it was found that 20° was the lowest angle that gave reproducible and stable correlation functions. Indeed, this practice is conceptually similar to examples in the literature using moderately sized DNA (<2500 bp),[16,40] where both a "fast" and "slow" diffusive mode can be resolved at a scattering angle of 90° ($ql = 5.2$). In these cases, this proved sufficient to extract the slow mode translational diffusion coefficient from the scattering data.

Despite the challenges of determining the translational diffusion coefficient for λ-DNA in the expanded-coil state, this relatively large DNA macromolecule was utilized as a means of investigating the limits of the photoreversible DNA compaction technique, as well as purposefully choosing a DNA molecule of a size more realistic from gene delivery and biotechnology perspectives. Once in the condensed state, note that the effects of the fast modes from rotational and internal motions greatly diminish, simplifying measurement of the diffusion coefficient of compacted λ-DNA.

Photocontrol of DNA Condensation. The ability to control DNA compaction with light illumination is shown through diffusion coefficient measurements in Figure 3a as a function of azoTAB concentration. The more hydrophobic, trans (visible light) form of the surfactant has a greater affinity to bind to and therefore condense DNA than the relatively hydrophilic, cis (UV light) isomer. Although the main driving force for binding is due to electrostatic interactions between the polynucleotide and the surfactant, this experiment demonstrates the importance that surfactant hydrophobicity, along with potential steric differences between the planar and bent conformations, can have on DNA condensation (the precise binding mechanism will be considered in greater detail below in the section dealing with crystal violet spectral properties). Indeed, the ability of the azoTAB surfactant to condense DNA is determined by the trans or cis conformation, which in turn is determined by the wavelength of light illumination. Using this property, we are therefore able to control the condensation of DNA with simple light illumination.

Under visible light conditions, the diffusion coefficient of the DNA/surfactant complex begins to increase at an r-ratio of about 7, indicating a decrease in the overall size of the DNA/surfactant complex due to condensation. The measured diffusion coefficient steadily increases up to $r = 9$, beyond which an approximately constant value is obtained, indicating that at this point the majority of the DNA molecules are condensed. Since the condensation of DNA is generally described as a discrete phenomena,[4] (i.e., partial condensation does not occur), it is

(57) Mackay, R. A.; Letts, K.; Jones, C. In *Interactions and Reactions in Microemulsions*; Mittal, K. L., Ed.; Plenum: New York, 1977; pp 801−816.
(58) Lee, C. T., Jr.; Smith, K. A.; Hatton, T. A. Photoreversible viscosity changes and gelation in mixtures of hydrophobically modified polyelectrolytes and photosensitive surfactants. *Macromolecules* **2004**, *37*, 5397−5405.
(59) Pecora, R. Spectral distribution of light scattered by monodispersed rigid rods. *J. Chem. Phys.* **1968**, *48* (9), 4126−4128.
(60) Pecora, R. Spectral distribution of light scattered from flexible-coil macromolecules. *J. Chem. Phys.* **1968**, *49* (3), 1032−1035.
(61) Stellwagen, E.; Lu, Y.; Stellwagen, N. C. Unified description of electrophoresis and diffusion for DNA and other polyions. *Biochemistry* **2003**, *42*, 11745−11750.
(62) Widom, J.; Baldwin, R. L. Monomolecular condensation of λ-DNA induced by cobalt hexamine. *Biopolymers* **1983**, *22*, 1595−1620.

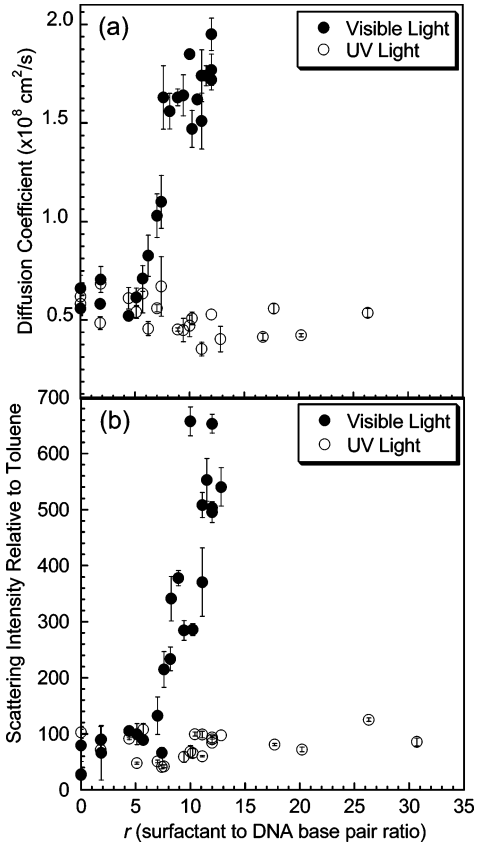

Figure 3. (a) Translational diffusion coefficient measurements of λ-DNA at 20° as a function of the surfactant-to-DNA base pair ratio. Closed symbols indicate diffusion coefficients measured under visible light, while open symbols are those obtained for the same solutions under UV light. [λ-DNA] = 0.05 mM, T = 25 °C. DNA compaction is observed under visible light beyond an r-ratio of about 7. (b) Relative scattering intensity of λ-DNA solutions to toluene, corresponding to the same solutions as in (a).

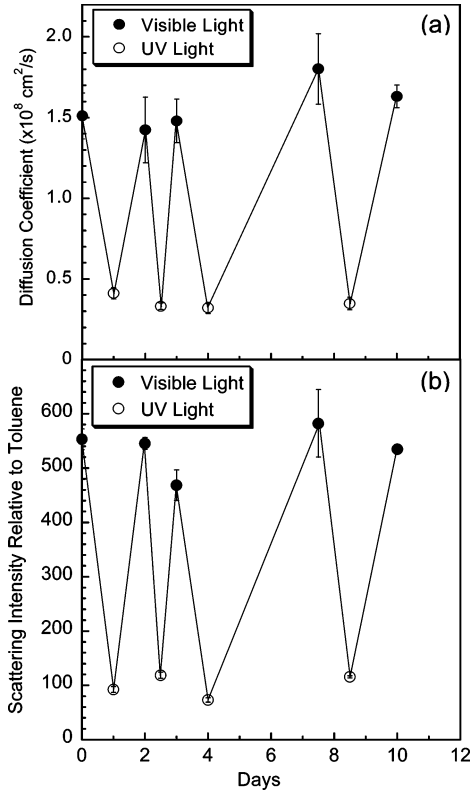

Figure 4. (a) Translational diffusion coefficient measurements of λ-DNA at a scattering angle of 20° at r = 11.5 as a function of time upon repeated visible/UV light cycles. [λ-DNA] = 0.05 mM, T = 25 °C. (b) Relative scattering intensity of λ-DNA to toluene for the same conditions as in (a).

expected that in the region $r = 7-9$, a mixture of compacted and elongated DNA molecules exist in equilibrium, with the value of the diffusion coefficient obtained representing an average between these two forms. Beyond an r-value of ~13 under visible light, the presence of aggregates start to dominate and the value of the diffusion coefficient start to decrease. The value of the diffusion coefficient obtained for DNA in a compacted state ($\sim 1.7 \times 10^{-8}$ cm^2/s) is similar to the value obtained for condensates of λ-DNA by polyamine homologues.[18] This illustrates a dramatic reduction in size of λ-DNA, from an end-to-end distance of 1.27 μm in the elongated-coil state to a hydrodynamic radius of approximately 120 nm in the compacted state.

Concurrently with the increase in the diffusion coefficient upon compaction, a large increase of the intensity of the scattered light is also observed, as shown in Figure 3b. Similar observations have been previously reported to occur upon DNA compaction, including λ-DNA condensed with polyamines.[15,17,18] At first glance, this phenomenon may appear counterintuitive, as it is well-known that scattering intensity varies as the square of particle volume (or equivalently as radius to the sixth power for spherical particles). Thus, a decrease in size is often accompanied by a decrease in scattering intensity. However, λ-DNA in the elongated state is of a size on the order of the wavelength of incident light (632.8 nm), which creates destructive intramolecular interference effects, as two parts of the same molecule may scatter light out of phase with each other.[14,40] As a result, the scattering intensity of DNA in the native state ($\langle R^2 \rangle^{1/2}$ = 1.27 μm) is much lower than that of DNA in the compact state (R_H = 120 nm), where interference effects are diminished. In addition, surfactant bound to DNA would increase the effective molecular weight of the scatterer, as well as neutralize DNA and thereby increase the attractive interactions between molecules, both of which could contribute to the increase in scattering intensity.

As shown in Figure 3, DNA condensed with surfactant under visible light can be induced to expand back to the native, elongated-coil conformation with UV light illumination. This phenomena is highlighted in Figure 4a, where over the course of 10 days a DNA−azoTAB solution at r = 11.5 was *photoreversibly* compacted and expanded through continuous and repeated visible/UV light exposure cycles.

The diffusion coefficients range from about $1.5-1.8 \times 10^{-8}$ cm^2/s under visible light and $\sim 0.4 \times 10^{-8}$ cm^2/s with UV light illumination, demonstrating excellent reproducibility and reversibility in such a complex system. Furthermore, these data combined with additional control experiments of measuring the absorbance of DNA at 260 nm (which would undergo an ~30% increase if the DNA strands unraveled) indicate that the photoreversible expansion and contraction of DNA does not damage the macromolecule. With DNA condensation using "traditional" (i.e., non-light-responsive) complexing agents, compaction can be reversed only through dilution of the complexing species.[4] In contrast, the photoreversible condensation of DNA shown in Figures 3 and 4 occurs at constant thermodynamic conditions (concentration, pH, etc.) representing

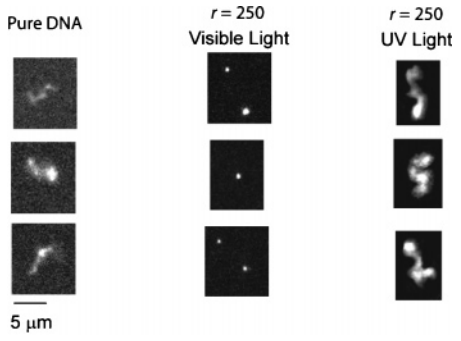

Figure 5. Fluorescence images of T4-DNA molecules in the elongated-coil conformation in TBE buffer solution, in the globular conformation upon addition of azoTAB surfactant ($r = 250$) under visible light, and the resulting reexpansion of DNA with UV light illumination. [T4-DNA] = 0.6 μM.

a novel method of studying DNA dynamics, and could eventually result in unique gene delivery and biotechnology applications.

Direct Detection of DNA Compaction. Fluorescence microscopy was used to visually observe conformational changes of T4-DNA induced by the addition of azoTAB surfactant and as a means to independently confirm the light-scattering results above.

Figure 5 shows fluorescence images of pure T4-DNA molecules in solution in the extended-coil formation (which were observed to exhibit translational, rotational, and internal motions, as described above). With the addition of azoTAB surfactant ($r = 250$) under visible light, however, the DNA molecules collapsed into small globules with no extended coils detected. Subsequent exposure of this solution to UV light for 30 min then resulted in a mixture of coils and small globules to be observed in solution, with selected coils shown in Figure 5. This proves the reversibility of the compaction process as the solution was mixed under visible light and then illuminated with UV light. It should be mentioned that this *r*-ratio required to induce full compaction under visible light is significantly higher than that required in the light-scattering experiments. For example, the use of lower *r*-ratios under visible light gave either no evidence of compaction ($r = 0-10$) or a mixture of expanded and compacted DNA ($r = 10-200$). This difference in the amount of surfactant required to induce condensation is a direct result of the relatively low DNA concentrations required for single-molecule detection with fluorescence microscopy (0.6 μM) compared to that used in the light-scattering experiments (50 μM). Similarly, *r*-ratios of 42, 160, and 600 using CTAB, TTAB, and DTAB, respectively, have been reported to be necessary to completely condense T4-DNA with microscopy.[63] This behavior can be explained from the fact that as the DNA concentration is reduced, higher *r*-ratios will be required to surpass the critical aggregation concentration, namely the surfactant concentration where the amphiphile begins to hydrophobically bind to (and thus condense) DNA.

Phase Behavior. Interactions between DNA and photosurfactant were further investigated and studied through the construction of DNA−azoTAB−water phase diagrams, as shown in Figure 6.

As expected for a mixture of a cationic surfactant and an oppositely charged polyelectrolyte, strong azoTAB−DNA interactions can eventually lead to an associative phase separation,[3,64] as the DNA complexes are neutralized with surfactant binding. Under both visible and UV light, the amount of surfactant necessary to result in DNA precipitation is found to be nearly independent of DNA concentration (note lower DNA concentrations similar to those used in the microscope experiments were not able to be tested, due to the visual method of detecting phase separation). Phase separation being nearly independent of surfactant concentration has been reported before in other DNA-based systems[3,65] and is also reminiscent of the behavior generally observed in surfactant−polyelectrolyte systems, where the critical aggregation concentration (CAC, i.e., the surfactant concentration where cooperative binding onto the polyelectrolyte begins to occur) has been found to be only a weak function of the polyelectrolyte concentration. Under UV illumination, it is found that phase separation requires about 3−4 times as much azoTAB as under visible light illumination. At the low DNA concentrations employed in the DLS experiments ([DNA] = 0.05 mM), the phase transition is seen to occur at approximately $r = 10$ under visible light exposure, similar to the surfactant-to-DNA ratio where condensation was observed in Figure 2, as expected as condensation via neutralization could be regarded as an initial step toward DNA aggregation and phase separation.

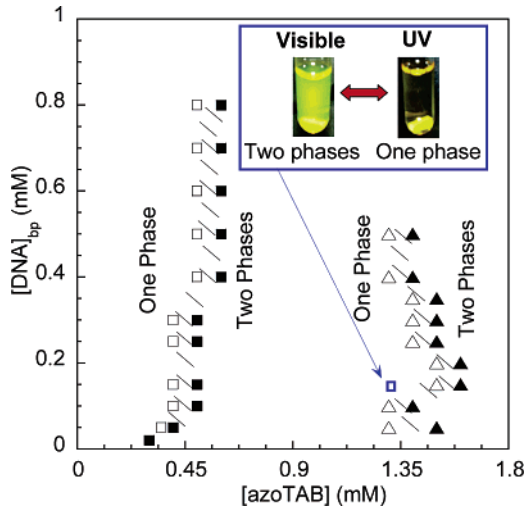

Figure 6. Phase behavior of the herring testes DNA−azoTAB−H_2O pseudoternary system. Open symbols represent the last one-phase solution and closed symbols the first two-phase solution observed upon increasing surfactant concentration. Squares represent data obtained under visible light, while triangles are used for data obtained under UV light. Pictures show a solution at [HT-DNA] = 0.15 mM and [azoTAB] = 1.3 mM in H_2O under visible (two phases) and UV (one phase) light.

Together, the observations of a CAC-type behavior along with light-controlled DNA condensation indicate that the observed phase separation is not entirely controlled by electrostatic interactions. Indeed, hydrophobic effects appear to play an important role, with the more hydrophilic cis conformation of the surfactant showing a lower tendency to precipitate DNA than the relatively hydrophobic trans isomer. Similar phase transitions have been observed in mixtures of DNA with

(63) Dias, R. S.; Pais, A. A. C. C.; Miguel, M. G.; Lindman, B. DNA and surfactants in bulk and at interfaces. *Colloids Surf., A* **2004**, *250*, 115−131.

(64) Thalberg, K.; Lindman, B.; Karltröm, G. Phase diagram of a system of cationic surfactant and anionic polyelectrolyte: Tetradecyltrimethylammonium bromide−hyaluronan−water. *J. Phys. Chem.* **1990**, *94*, 4289−4295.

(65) Guillemet, F.; Piculell, L. Interactions in aqueous mixtures of hydrophobically modified polyelectrolyte and oppositely charged surfactant. Mixed micelle formation and associative phase separation. *J. Phys. Chem.* **1995**, *99*, 9201−9209.

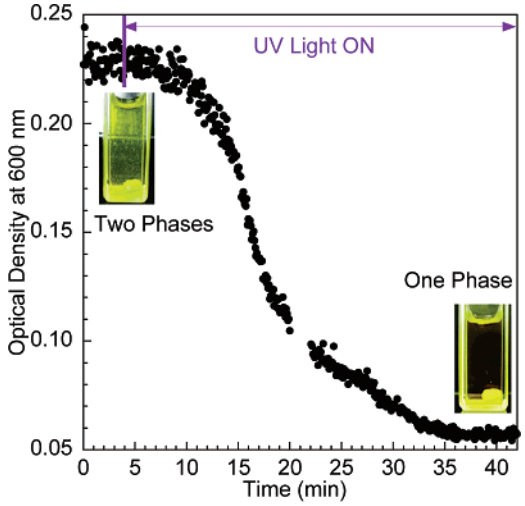

Figure 7. Kinetics of dissolution of an azoTAB−DNA precipitate under constant stirring upon UV light illumination for [HT-DNA] = 0.15 mM and [azoTAB] = 1.3 mM in H_2O. The stir bar used to mix the samples during the experiment can be observed at the bottom of the cuvettes.

traditional alkyl-based trimethylammonium bromide surfactants, including C_{12}TAB, C_{14}TAB, and C_{16}TAB, where increasing the length of the hydrocarbon tail (i.e., making the surfactant more hydrophobic) leads to phase separation at lower surfactant concentrations.[3] In the case of Figure 6, however, this hydrophobic effect and the resulting phase transition are entirely light initiated.

The photocontrol of DNA phase separation is further demonstrated in Figure 7, where the optical density at 600 nm (which is far removed from the surfactant absorbance shown in Figure 1, thereby solely giving a measure of solution turbidity) of a phase-separated DNA solution equilibrated under visible light is shown following exposure to UV light.

Dissolution of the precipitate as the surfactant is converted to the cis form is found to occur in ∼35 min, generally fast given the high molecular weight of DNA. Furthermore, exposure of the now one-phase, UV light equilibrated solution to visible light results in re-formation of the precipitate over several hours (not shown), due to the relatively slow nucleation process. Throughout several precipitation−dissolution cycles, the absorbance of DNA at 260 nm did not increase, indicating that there was no DNA strand separation. Thus, the phase transitions, as in the DNA condensations shown above with light scattering, are completely photoreversible.

Fluorescence and Absorbance of Crystal Violet. To elucidate the binding mechanisms of azoTAB with DNA, the cationic probe crystal violet was used to report on the binding state of the surfactant. Crystal violet is a *micropolarity* probe with an absorption maximum that depends on the environment in which the molecule is located. In a polar solvent such as water, λ_{max} = 590 nm, while in a nonpolar solvent such as benzene, λ_{max} = 605 nm.[57] A similar bathochromic shift from λ_{max} = 590 nm to λ_{max} = 593 nm has also been reported upon binding of crystal violet to DNA, accompanied by a decrease in the absorbance of the probe related to an increase in the degree of deformation of the phenyl rings about the central carbon from a propeller to a more planar conformation, a result of π-stacking as crystal violet forms aggregates along the surface

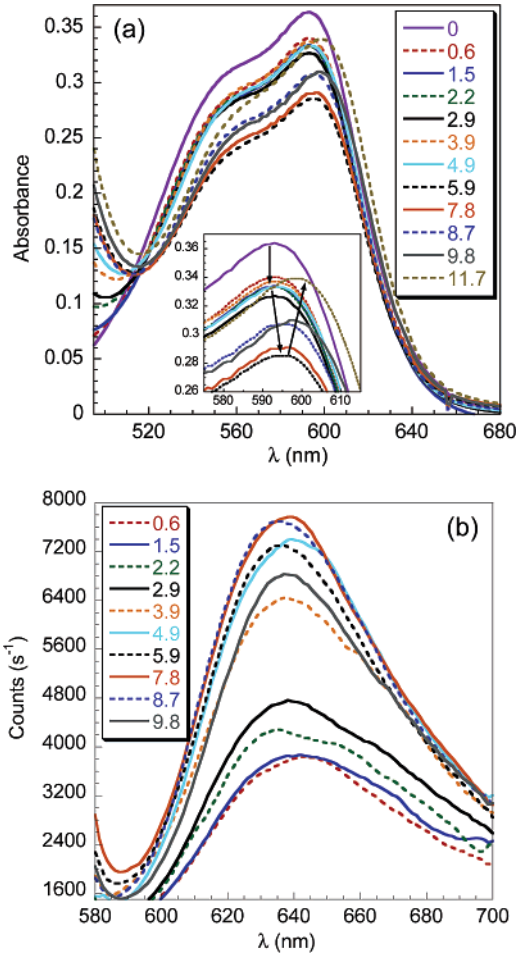

Figure 8. (a) Absorption and (b) fluorescence emission spectra of crystal violet as a function of the azoTAB-to-DNA base pair ratio under visible light only. [HT-DNA] = 40.8 μM, [CV] = 5.2 μM, λ^{ex} = 570 nm.

of DNA.[66] Used as a fluorescent probe, crystal violet is also a well-known *microviscosity* indicator with a fluorescence emission that increases as the rotational relaxation of the aromatic rings becomes hindered, such as upon binding to proteins.[67] Therefore, by analyzing the absorbance and fluorescence emission spectra of crystal violet upon addition of azoTAB to DNA solutions, information on the local polarity and "viscosity" experienced by the probe can be obtained and thereby used to infer details of the azoTAB binding process.

Figure 8a shows the variation of the absorbance of crystal violet in DNA mixtures upon addition of azoTAB surfactant under visible light. Upon binding to DNA, a shift in λ_{max} of crystal violet from the aforementioned 590 nm in water to 593 nm is observed, similar to previous values obtained in pure DNA solutions.[66] This value of λ_{max} persists below r = 3.9, as apparently the concentration of bound surfactant is too low to induce polarity changes in crystal violet. Over the region from r = 3.9 to r = 5.9, however, the addition of surfactant produces a red shift in λ_{max} from 593 to 595 nm, indicating that crystal violet is experiencing a less polar microenvironment, while at the same time a decrease of absorbance is observed, potentially a result of π-stacking of crystal violet with the benzene rings

(66) Wakelin, L. P. G.; Adams, A.; Hunter, C.; Waring, M. J. Interaction of crystal violet with nucleic acids. *Biochemistry* **1981**, *20*, 5779−5787.
(67) Baptista, M. S.; Indig, G. L. Effect of BSA binding on photophysical and photochemical properties of triarylmethane dyes. *J. Phys. Chem. B* **1998**, *102* (23), 4678−4688.

of the surfactant bound to DNA. Note that these changes occur over *r*-ratios where the DLS results have yet to detect condensation. This is not surprising, as the DLS technique provides information on changes occurring to DNA molecules as a whole (i.e., expanded or compacted), whereas crystal violet probes (and is very sensitive to) changes in the local environment surrounding the molecule. Thus, it is likely that crystal violet detects the initial onset of binding of azoTAB to DNA that eventually leads to condensation. Interestingly, above $r = 5.9$ further addition of surfactant now induces an increase in crystal violet absorbance as well as a further red shift up to $\lambda_{max} = 598$ nm, showing an easing of the effects of π-stacking and a decrease in the polarity of the local environment, respectively. Note that under UV light illumination, λ_{max} remains at 592 nm for all the solutions studied in Figure 8 (results not shown), indicating that the cis form of the surfactant does not interact with crystal violet (and hence DNA) over these concentration ranges.

The fluorescence emission of crystal violet under visible light shown in Figure 8b displays similar trends as observed in Figure 8a. With the addition of surfactant, the fluorescence intensity steadily increases up to an *r*-ratio of ~7.8−8.7, demonstrating an increase of the local viscosity (or equivalently a decrease in molecular flexibility) experienced by crystal violet, again prior to dramatic changes in DNA conformation detected with DLS. These results agree with previous observations that a stacked arrangement of crystal violet with azoTAB could be responsible for the decrease of the molecular flexibility of the benzene rings of crystal violet. For higher surfactant concentrations, however, the fluorescence emission decreases, representing a decrease in the restriction of the rotation of the benzene rings of crystal violet around the central carbon.

Comparison of these spectroscopic results with the DLS data in Figure 2 provides insight into the DNA compaction process that begins to occur at approximately $r = 7$. Apparently, the condensed DNA molecules provide a more hydrophobic region where crystal violet molecules become solubilized (increase in λ_{max}) and are subject to less steric effects of π-stacking (increase in absorbance), which allows the aromatic rings of crystal violet to rotate more freely about the central carbon (decrease in fluorescence). These results are consistent with the idea that azoTAB-condensed DNA potentially exists as toroids, with crystal violet bound between subsequent DNA layers.

Furthermore, the observed changes in crystal violet absorbance and fluorescence in Figure 8 can be used to indirectly probe the binding mechanism of azoTAB with DNA. The continual increase in the λ_{max} of crystal violet with the addition of surfactant beyond $r = 3.9$ indicates that crystal violet is experiencing an increasingly less polar environment over this region, likely a result of crystal violet and azoTAB beginning to interact at this *r*-ratio. This is further supported by the decrease in the absorbance of crystal violet over similar *r*-ratios, which as mentioned above is often associated with π-stacking of crystal violet. Together, these two observations point to a "tail−tail" type of interaction between the phenyl groups of azoTAB and crystal violet that are bound to adjacent sites on DNA. This is also consistent with the steady increase in the fluorescence emission of crystal violet with surfactant concentration, indicating a hindrance to the rotational relaxation of the aromatic rings of crystal violet. Apparently, while the ionic headgroups of the surfactant molecules are bound to DNA, the surfactant tails undergo hydrophobic interactions with crystal violet, potentially leading to stacking along the DNA chain. On the basis of this argument, it appears that neither crystal violet nor azoTAB are intercalated within the DNA base pairs. Furthermore, this type of interaction between crystal violet and azoTAB could be thought to mimic the type of hydrophobic interactions between surfactant molecules that would induce the cooperative binding regime and lead to DNA condensation.

Conclusion

The ability to reversibly control DNA condensation using light illumination has been demonstrated through the use of a photoresponsive azoTAB surfactant as the compacting agent. Addition of the surfactant to DNA solutions under visible light (where azoTAB adopts a relatively hydrophobic trans conformation) causes the diffusion coefficient of λ-DNA to increase from a value of 0.6×10^{-8} cm^2/s for the elongated-coil state (end-to-end distance of 1.27 μm) to a value of approximately 1.7×10^{-8} cm^2/s for DNA in the compact state (hydrodynamic radius of 120 nm). Exposure of these same compacted solutions to UV light (where azoTAB adopts a relatively hydrophilic cis conformation) causes DNA to expand to the elongated coil. The condensation process was further demonstrated to be completely photoreversible by measuring the DNA−azoTAB sample over the course of 10 days with repeated visible/UV light cycles. Moreover, direct images of T4-DNA obtained with fluorescence microscopy indicated that DNA globules obtained at high surfactant concentrations under visible light could be transformed to the elongated-coil state following UV light illumination. Results from additional phase behavior and spectroscopic experiments demonstrate the importance of both electrostatic and hydrophobic forces in the compaction process. As a result, with the use of a surfactant with light-responsive hydrophobicity, DNA condensation can be reversibly controlled with simple light illumination.

Acknowledgment. We would like to acknowledge the Charles Lee Powell Foundation and the James H. Zumberge Faculty Research And Innovation Fund for support for this research. We also thank Jing Zhang, Bartley Gill, and Hong Wong for their contributions.

JA0576738